NJC

Accepted Manuscript

This is an *Accepted Manuscript*, which has been through the Royal Society of Chemistry peer review process and has been accepted for publication.

Accepted Manuscripts are published online shortly after acceptance, before technical editing, formatting and proof reading. Using this free service, authors can make their results available to the community, in citable form, before we publish the edited article. We will replace this *Accepted Manuscript* with the edited and formatted *Advance Article* as soon as it is available.

You can find more information about *Accepted Manuscripts* in the Information for Authors.

Please note that technical editing may introduce minor changes to the text and/or graphics, which may alter content. The journal's standard Terms & Conditions and the Ethical guidelines still apply. In no event shall the Royal Society of Chemistry be held responsible for any errors or omissions in this *Accepted Manuscript* or any consequences arising from the use of any information it contains.

ROYAL SOCIETY OF CHEMISTRY

www.rsc.org/njc

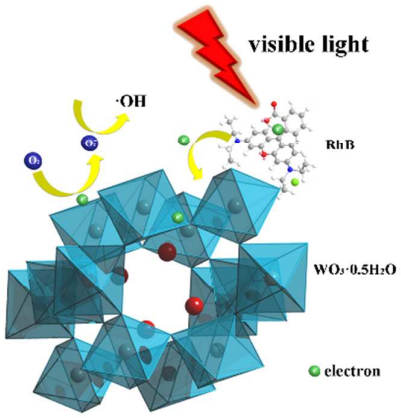

$$Dye \xrightarrow{h\nu} Dye^{*}$$

$$UWAT\text{-}1 \xrightarrow{h\nu} e^{-}_{CB} + h^{+}_{VB}$$

$$Dye^{*} + UWAT\text{-}1 \longrightarrow Dye^{+} + UWAT\text{-}1^{e^{-}_{Dye}}$$

$$e^{-} + O_2 \longrightarrow O_2^{\bullet -}$$

$$O_2^{\bullet -} \xrightarrow{\text{protonation}} {}^{\bullet}OOH \xrightarrow{H^{+}+e^{-}} {}^{\bullet}OH + OH^{-}$$

$$h^{+} + OH^{-} \longrightarrow {}^{\bullet}OH$$

$$h^{+} + H_2O \longrightarrow {}^{\bullet}OH + H^{+}$$

$$Dye + \{ O_2^{\bullet -}, {}^{\bullet}OH \} \longrightarrow \text{final substrates}$$

Solvothermal synthesis of c-$WO_3 \cdot 0.5H_2O$ with high photocatalytic activity

Journal Name

RSCPublishing

ARTICLE

Solvothermal synthesis of pyrochlore-type cubic tungsten trioxide hemihydrate and high photocatalytic activity †

Cite this: DOI: 10.1039/x0xx00000x

Received 00th January 2012,
Accepted 00th January 2012

DOI: 10.1039/x0xx00000x

www.rsc.org/

Yi Zheng, Gang Chen,* Yaoguang Yu, Yu Wang, Jingxue Sun, Haiming Xu, and Yansong Zhou

Pyrochlore-type cubic phase tungsten trioxide hemihydrate (c-WO_3·0.5H_2O) has been synthesized firstly via a simple solvothermal process. The photocatalytic property has been investigated firstly by photodegradation of RhB, c-WO_3·0.5H_2O sample performed high photocatalytic activity, indicating that c-WO_3·0.5H_2O is a promising candidate of tungsten oxide-based photocatalytic materials. The investigation result of the crystal water effects on photocatalytic activity showed that crystal water of c-WO_3·0.5H_2O played a key role on photocatalytic activity. The novel method reported in this study has a great potential for the development of tungsten trioxide-based functional material preparation to improve their photocatalytic efficiency in elimination of hazardous substances applications, as well as the energy materials.

Introduction

Tungsten trioxide as an important inorganic material, has received a lot of attentions because of their strong potential applications in various fields such as electrochromism, [1, 2] photochromism, [3, 4] lithium battery, [5, 6] and gas sensor. [7, 8] Especially, tungsten trioxide has attracted much interest in photocatalytic application due to its relatively small bandgap (E_g ~ 2.6 eV), which could theoretically utilize about 12% solar light.[9, 10].

The photocatalytic property of tungsten trioxides is influenced by some factors, such as morphology, [11, 12] doping, [13-16] composite, [17-19] and exposed facet [20, 21] *etc*. In particular, composition and crystal structure are also important and direct influence factors. [19, 22-26] For example, Yu *et al.* studied photocatalytic properties of orthorhombic WO_3·H_2O and monoclinic WO_3, WO_3·H_2O has enhanced photocatalytic property compared to WO_3. [23] Shi *et al.* reported photodegration of methylene blue over hexagonal WO_3, orthorhombic WO_3·0.33H_2O, and cubic WO_3·0.5H_2O, wherein WO_3·0.5H_2O displays the best performance. [22] From examples, it can be seen that hydrated tungsten trioxide may have more excellent photocatalytic property compared with tungsten trioxide itself. But few reports about the photocatalytic property of tungsten trioxide hydrates were reported, particularly for c-WO_3·0.5H_2O. There are some articles on their synthesis only,[22, 27-31] but the study on photocatalytic property of c-WO_3·0.5H_2O have been neglected. Therefore, it is necessary to study the synthesis method of c-WO_3·0.5H_2O and its photocatalytic property. In previous study, the c-WO_3·0.5H_2O are all synthesized in water.

In this work, we have firstly synthesized an efficient visible-light-driven photocatalyst in terms of cubic tungsten trioxide hemihydrate, which could be facilely obtained via a solvothermal method. In addition, the photocatalytic property of c-WO_3·0.5H_2O has been investigated. The c-WO_3·0.5H_2O performs high photocatalytic activity for the photodegradation of Rhodamine B under visible-light illumination. Further study showed that crystal water of c-WO_3·0.5H_2O played a key role on photocatalytic activity. To the best of our knowledge, synthesis of c-WO_3·0.5H_2O via solvothermal method have not been investigated yet. The novel method reported in this study has a great potential for the development of tungsten trioxide-based functional material preparation to improve their photocatalytic efficiency, as well as the energy materials.

Experimental

Materials

Sodium tungstate dihydrate (Na_2WO_4·2H_2O, AR) of ≥ 99.5% purity was purchased from Sinopharm Chemical Reagent Co., Ltd. Urea (CH_4N_2O) of > 99% purity was purchased from Aladdin Inc. Hydrochloric acid and acetone are analytical reagent purchased from Sinopharm Chemical Reagent Co., Ltd.

Synthesis of c-WO_3·0.5H_2O

Na_2WO_4·2H_2O (0.5 g, 1.516 mmol) and urea (0.1 g, 1.665 mmol) were dissolved in 11 mL, 16.5 mL, 22 mL of ultra-pure water at room temperature. 0.43 mL of 38% HCl was added slowly and carefully, a bit yellow clear H_2WO_4 collosol was obtained, and then 22 mL, 16.5 mL, 11 mL of acetone was added correspondingly. Then above solution was placed into a Teflon-lined stainless steel autoclave, which was sealed and maintained at 140 °C for 72 h, then rinsed with deionized water several times and dried at 60 °C, we called it UWAT-1, UWAT-2, UWAT-3, respectively. And UAT was synthesized by adding Na_2WO_4·2H_2O (0.5 g, 1.516 mmol), urea (0.1 g, 1.665 mmol), 33 mL acetone and 0.43 mL of 38% HCl successively and directly into Teflon-lined stainless steel autoclave and then rinsed with deionized water several times and dried at 60 °C. Anhydrous c-WO_3 was obtained by dehydration at 200 °C 3h, and new c-WO_3·0.5H_2O was obtained by hydrothermal process with water only at 180°C 22h.

Characterization

The collected products were characterized by powder X-ray diffractometer (Rigaku D/max-2000) with Cu Kα radiation at a scanning rate of 5° min^{-1} in the 2θ range of 10°–90°, The morphology of the products were observed by FESEM (Helios Nanolab600i), TEM and HRTEM were carried out on FEI TecnaiG2F30, UV–vis diffuse reflectance spectra were acquired by a spectrophotometer (TU-1900) and $BaSO_4$ was used as the reflectance standard.

Photocatalytic activity measurement

In this measurement, a 300W Xe lamp (Trusttech PLS-SXE 300, Beijing) with a cut-off filter (λ > 400 nm) was used as light source, and 10 mg·L^{-1} RhB aqueous solution, as a representative compound, was used as target photodegradation pollutant in heterogeneous photocatalysis reaction. In each experiment, a quartz beaker containing 100 ml RhB aqueous solution and 50 mg photocatalyst was firstly put into an ultrasonic bath to disperse photocatalyst under dark 10 min, and then stirred 40 min in dark continuously in order to achieve adsorption–desorption equilibrium. The concentration of RhB during the degradation process was monitored by colorimetry using a UV-vis spectrometer (TU-1900) every 20 min, which obtained by being centrifuged at 10,000 rpm for 5 min.

Results and discussion

Phase composition and microstructure

Cubic tungsten trioxide hemihydrates (c-WO_3·0.5H_2O) have been synthesized via solvothermal with adding urea. The products was named as UWATs and UAT, as seen in Tab. 1.

The phase of the as-prepared tungsten trioxide hemihydrates were examined by X-ray diffraction in Fig. 1. The diffraction peaks of cubic tungsten trioxide hemihydrates (Fig. 1a-d) are in good agreement with the standard data of c-WO_3·0.5H_2O

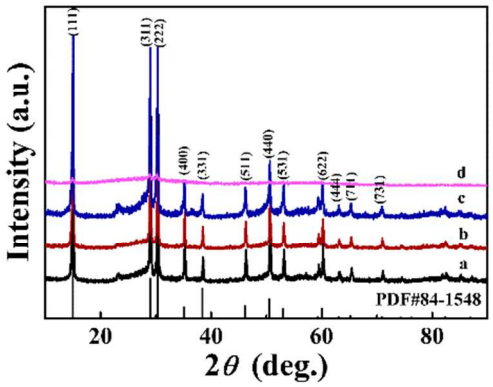

Fig. 1 X-ray diffraction (XRD) patterns of tungsten trioxide hemihydrates prepared in mixed solvent (water : acetone) in different volume ratio (a) 2 : 1, (b) 1 : 1, (c) 1 : 2, (d) only acetone used as solvent.

Tab. 1 The short name of synthesized cubic tungsten trioxide hemihydrates with different synthesis conditions.

	urea	water	acetone
UWAT-1	0.1 g	11 mL	22 mL
UWAT-2	0.1 g	16.5 mL	16.5 mL
UWAT-3	0.1 g	22 mL	11 mL
UAT	0.1 g	0	33 Ml

(JCPDS card no. 84-1548) with lattice parameters a = 10.206 Å, and no other impurities were detected. The sharp peaks indicated the as-synthesized products were well-crystallized. But the UAT which was synthesized by using acetone as solvent only had very low diffraction peaks, which indicated that UAT is poor-crystallized. And poor crystallization will induce poor photocatalytic property. It may be due to many effect factors. Such as, poor crystallization may cause more defect, defect may act as recombination centers of the photo-generated electron–hole pairs. Poor crystallization may cause larger adsorption of dye, larger adsorption of dye may reduce the effective light-absorbing of semiconductor, *etc*.

Most researches have shown that pH is a key role for the crystal structure of the tungsten oxides, because different pH could impact the existing state of tungstate ion. [32-34] Günter found a new phase of cubic tungsten trioxide hemihydrate by regulating the pH of the solution to 3. [28] Reis also controlled solution pH between 3.5~4.5, and pyrochlore cubic WO_3 was obtained. [35] In the study of Li, pyrochlore cubic WO_3 have been gotten from different initial pH of solution, but the final pH of the solution is in the range of 7.0-8.5. Li believed the precipitation of c-WO_3·0.5H_2O occurred mainly in the pH range of 7.0 to 8.5. [31]

Investigations have shown that pH can affect the existence form of tungstate ions, and the various existence form of tungstate ions are considered to be the precursors of tungsten oxides with different crystal structure. In order to know the effect of pH, pH change experiments were carried out by adjusting the amount of hydrochloric acid. The pH was adjusted to 8, 7, 4, 2, 1.5, 1, respectively. When the pH was adjusted to 8 or 7, there was no product. When pH was adjusted to 4, there was very little product of c-$WO_3 \cdot 0.5H_2O$. When pH was adjusted to 2 or 1.5, there was product of c-$WO_3 \cdot 0.5H_2O$. When pH was adjusted to 1, the product changed into orthorhombic $WO_3 \cdot 0.33H_2O$. The XRD pattern were shown in Fig. S3. It is showed that pH affect the crystal structure of tungsten trioxide. In this work, c-$WO_3 \cdot 0.5H_2O$ would be obtained in the range of pH 4-1.

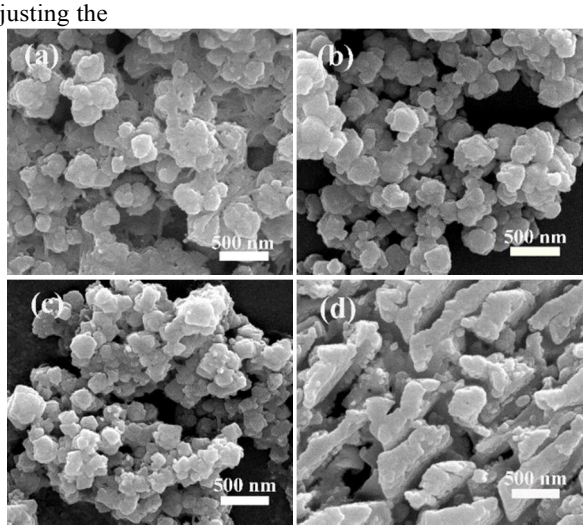

Fig. 2 SEM images of tungsten trioxide hemihydrates prepared in mixed solvent (water : acetone) in different volume ratio (a) 2 : 1, (b) 1 : 1, (c) 1 : 2, (d) only acetone used as solvent.

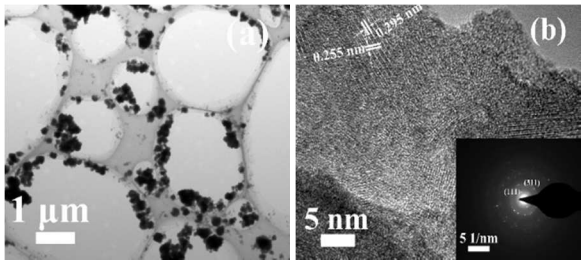

Fig. 3 TEM images of UWAT-1.

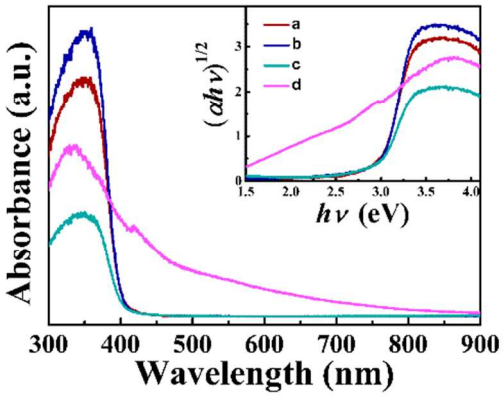

Fig. 4 UV–visible absorption spectra of tungsten trioxide hemihydrates prepared in mixed solvent (water : acetone) in different volume ratio (a) 2 : 1, (b) 1 : 1, (c) 1 : 2, (d) only acetone used as solvent.

Shi got c-$WO_3 \cdot 0.5H_2O$ by adjusting the amount of sodium sulfate without adjusting pH of solution. [22] Su respectively used equal amounts of L(+)-tartaric acid and citric acid as assistantagents and adjusted the initial pH of solution to 1 by hydrochloric acid, and accordingly to obtain hexagonal phase and orthorhombic phase of tungsten trioxide. [36] This shows that the chemical composition in the solution can also impact on the crystal structure except the factor of pH. Generally, nucleation is an important stage during crystallization process. I believe that chemical environment of the solution, including hydrogen ion concentration and other chemical components, plays a key role on nucleation stage.

The above two factors are both likely to exist. On one hand, acetone can occur condensation reaction with urea under acid condition (hydrochloric acid). [37, 38] Or reacts with urea and hydrochloric acid at the same time. The situation is more complex under solvothermal condition. Anyway, the pH of reaction system, which determine the crystal structure of tungsten oxide, could be changed. On the other hand, the reaction products of acetone, urea, and hydrochloric acid might also affect the crystal structure. The overall result is that c-$WO_3 \cdot 0.5H_2O$ is generated in such reaction system. More details about the nucleation process will be investigated in the future in-depth study.

The morphologies of the produced nanostructures were characterized by scanning electron microscopy (SEM), as shown in Fig. 2. The morphologies of cubic tungsten trioxide hemihydrate aggregated nanoparticles did not change significantly (Fig. 2a-c), except UAT (Fig. 2d). It can be speculated that photocatalytic properties of cubic tungsten trioxide hemihydrates could be similar, except UAT.

The TEM observations of c-$WO_3 \cdot 0.5H_2O$ also revealed the morphology. The size of c-$WO_3 \cdot 0.5H_2O$ aggregated nanoparticles were 120 nm – 180 nm. HRTEM image of c-$WO_3 \cdot 0.5H_2O$ indicated that the lattice spacing of 0.295 nm and0.255 nm are in good agreement with the (222) and (400) planes (Fig. 3d), which agrees well with the results by Nedjar *et al.* [27] But (111) and (311) planes were observed by selected area electron diffraction (SAED) patterns. However, (111) planes are equivalent plane to (222) planes, and the lattice spacing $d_{(111)}$ is equal to two times of $d_{(222)}$.

Optical properties

UV–visible absorption spectra revealed that the absorption edge of as-prepared c-$WO_3 \cdot 0.5H_2O$, and the band gap E_g was obtained by using the equation: $\alpha h\nu = A(h\nu - E_g)^n$, where α is absorption coefficient, h is Planck's constant, ν is the frequency

of light, A is a constant, and n is equal to 2 because WO_3 is indirect semiconductor. [39] So band gap energy will be obtained from the graph with $(\alpha h\nu)^{1/2}$ plotted as a function of $h\nu$. It is found that the band gap value for UWAT-1, UWAT-2, UWAT-3 was about 2.98 eV, 2.98 eV, 2.95 eV respectively. Whereas, E_g of UAT is 1.93 eV.

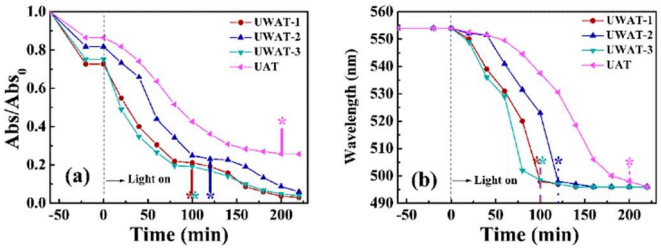

Fig. 5 Photodegradation profiles of RhB over UWATs (a) and corresponding maximum absorption wavelength change of organic substances (b) after visible light irradiation ($\lambda > 400$ nm).

Visible-light photocatalytic activity

Photocatalytic activities of cubic tungsten trioxide hemihydrates have been firstly investigated by choosing the photodegradation of RhB as a model reaction, to demonstrate the potential application of cubic tungsten trioxide hemihydrates in the photodegradation of organic contaminants. P25 and commercialtungsten trioxide were used as references. Compared to the photodegradation of RhB with references (Fig. S1), the as-prepared tungsten trioxide hemihydrates exhibited a remarkable photocatalytic activity of eliminating RhB. Fig. 5a showed the photodegradation curve of RhB solutions in the presence of the cubic tungsten trioxide hemihydrates under visible illumination, and the time-dependent absorption spectra of the RhB solution were shown in Fig. S2. The absorbance decreases by ca. 16% – 27% is the dark-adsorption of UWATs (c-WO_3·0.5H_2O). When visible light ($\lambda > 400$ nm) irradiated with the aqueous RhB/UWATs dispersion, it caused a decrease in intensity of absorption peak with a concomitant the maximum absorption wavelength of RhB shift to shorter wavelength, reminiscent of similar hypsochromic shifts can be seen by Watanabe *et al* [40] in the RhB/CdS system.

Because of the two kinds of spectral changes in photodegradation reaction, using the intensity of maximum absorption peaks and the maximum absorption wavelength as function of time to judge the photodegradation efficiency is more appropriate. The trend in overall diminution of the absorbance with increasing irradiation time is illustrated in Fig. 5a, and the trend of hypsochromic shifts during the photodegradation process is depicted in Fig. 5b. The asterisks in Fig. 5 represented the time required of complete de-ethylation.

The mentioned wavelength shift is due to de-ethylation of RhB which is caused by one of the active oxygen species attack on the N-ethyl group, [41] and it is inferred that the electron transferred from the singlet excited state $^1RhB^*$ to photocatalysts. [40] In addition, the de-ethylation process is in a stepwise manner, and the relationship between maximum absorption wavelength and organic dyes is that the maximum absorption wavelength of N,N,N',N'-tetraethylated rhodamine is 554 nm; N,N,N'-triethylated rhodamine, 539 nm; N,N'-diethylated rhodamine, 522 nm; N-ethylated rhodamine, 510 nm; and maximum absorption wavelength of rhodamine (rhodamine 110) is 498 nm, which can be known in Fig. 5b and Fig. S2. During the initial period of photodegradation of RhB, competitive reactions between de-ethylation and cycloreversion of the RhB occur, and de-ethylation is predominating. In de-ethylation process, the de-ethylation rate of RhB over UWAT-1 and UWAT-3 is slightly faster than UWAT-2, except UAT. The split ring rate of rhodamine 110 over UWAT-1 and UWAT-3 is also slightly faster than UWAT-2, which is indicated by changes in peak intensity at 498 nm. In the total photodegradation tests, UWAT-1 and UWAT-3 performed best photocatalytic activity in both de-ethylation process and cycloreversion pocess. However, among cubic tungsten trioxides, the photocatalytic properties are similar, which can be understood by the similar morphology and size from SEM images. But UAT is an exception, because of poor crystallinity and big size, which can be seen from XRD data (Fig. 1) and SEM image (Fig. 2).

In order to investigate the impact of crystal water to c-WO_3·0.5H_2O on its photodegradation property. Dehydration treatment to c-WO_3·0.5H_2O was carried out at 200℃, which was based on the research of Nedjar. [27] Nedjar said that anhydrous c-WO_3 can add water to form c-WO_3·0.5H_2O again at 140℃. [27] To possibly revert back water into c-WO_3·0.5H_2O, we choose 180℃ and utilize hydrothermal method to inject water into anhydrous c-WO_3. After 22h hydrothermal process, we obtained the new c-WO_3·0.5H_2O. The XRD pattern of anhydrous c-WO_3 is similar to c-WO_3·0.5H_2O, as shown in Fig. 6. But X-ray diffraction peaks shift to small angle, indicating that the lattice spacing of anhydrous cubic tungsten trioxide becomes large. This may be

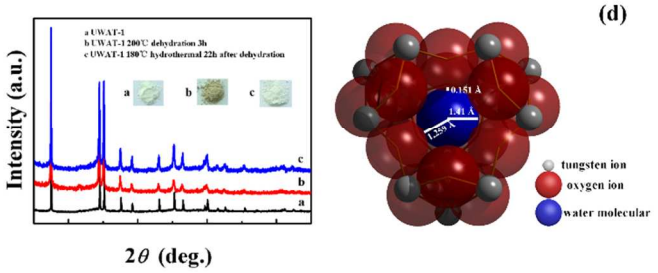

Fig. 6 X-ray diffraction (XRD) patterns of tungsten oxides, (a) UWAT-1, (b) UWAT-1 200℃ dehydration 3h, (c) UWAT-1 180℃ hydrothermal 22h after dehydration, (d) c-WO_3·0.5H_2O crystal structure

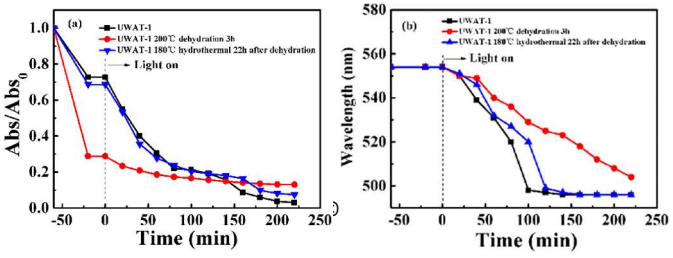

Fig. 7 Photodegradation profiles of RhB over UWAT-1, dehydrated UWAT-1, and new UWAT-1 (a) and corresponding maximum absorption wavelength change of organic substances (b) after visible light irradiation ($\lambda > 400$ nm).

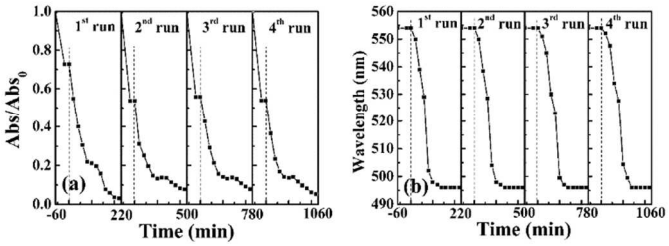

Fig. 8 Recycled photodegradation of RhB under the irradiation of visible light over UWAT-1.

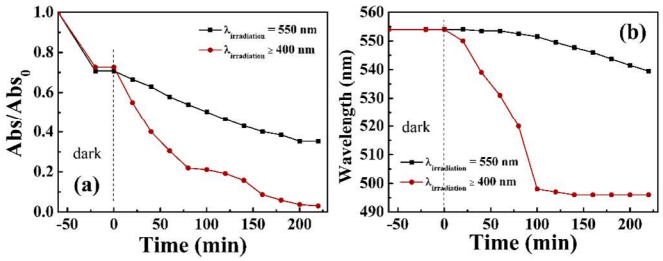

Fig. 9 Photodegradation profiles of RhB over UWAT-1 (a) and corresponding maximum absorption wavelength change of organic substances (b) after visible light (λ>400 nm) and 550 ± 15 nm monochromatic light irradiation.

caused by dehydration, because the size of water molecule (radius is 1.41 Å) is slightly larger than the tunnel pore of c-WO_3·0.5H_2O (radius is 1.259 Å), as shown in Fig. 6d. So water molecules might slightly enlarged the tunnel pores during the dehydration process. In Fig. 6, it can also be seen that the X-ray diffraction peaks of new c-WO_3·0.5H_2O (after adding water) shift to large angle compared to anhydrous c-WO_3, but compared to old c-WO_3·0.5H_2O the X-ray diffraction peaks is still blue shift. It may be induced by the crystal water could effect on the XRD peaks position. After photodegradation experiment, it is found that the photocatalytic activity of anhydrous c-WO_3 was very poor (Fig. 7 red circle). And the result of photodegradation experiment of new c-WO_3·0.5H_2O showed that new c-WO_3·0.5H_2O performed the similar photocatalytic activity (Fig. 7 blue inverted triangle) compared with old c-WO_3·0.5H_2O (Fig. 7 black square). It is showed that crystal water played a key role on the excellent photocatalytic activity of c-WO_3·0.5H_2O. Fig. S3 showed that the crystal structure of UWTA-1 didn't changed after photodegradation of RhB.

The reason why hydrate enhanced the photocatalytic properties is complex and unknown. A possible conjecture was proposed, the conjecture is that the crystal water was located in cages which were composed of W and O and these cages adjoined with each other. The size of crystal water is slight less than the cages, and crystal water may form hydrogen bonds with the O. Thus, the inside electron density of c-WO_3·0.5H_2O will maximize overlap, and form more and shorter carrier mobility access between the cages with each other which is shorter than the carrier mobility access composed of W and O. Thereby enhancing the photocatalytic activity. In this regard, it will do further studies in the future.

The stability is a very important role for practical application. In order to close to practical situation, the four cycles of photodegradation of RhB were carried out over cubic tungsten trioxide hemihydrate without stopping (Fig. 8). That means cubic tungsten trioxide hemihydrate powder wasn't got out, washed, and dried after every photodegradation experiment. We just removed the supernatant, and then added new dye solution for a new cycle experiment. In order to maintain the same experimental condition, few new dry cubic tungsten trioxide hemihydrate powder, which was obtained after once photodegradation experiment, were added at the beginning of every cycle experiment. Fig. 8a shows that the dark absorption of dye was increased after first run, this may be due to pulverization which can induced larger specific surface area. The performance didn't decrease obviously (just decreased less than 5%). Fig. 8b shows no obvious changes on de-ethylation process. These results all indicate that c-WO_3·0.5H_2O exhibits good stability and reusability.

From above results, c-tungsten trioxide hemihydrate is a good candidate for treating waste water, also due to it is noxious, green, stable, and inexpensive, especially its unique crystal structure.

Photolysis mechanism

The presence of dye-sensitized has been investigated firstly, because of RhB is colourful dye and may induce photosensitization. It can be known from experimental data, RhB can mainly absorb the light with wavelength 554 nm, and the c-WO_3·0.5H_2O just can absorb the light with wavelength shorter than 405 nm. So, the photodegradation experiment was carried out by using 550 ± 15 nm band-pass filter for exciting the RhB only, as shown in Fig. 9. Fig. 9a shows that 64.7% RhB can be decomposed when photodegradation experiment with 550 ± 15 nm band-pass filter was completed. It indicates that dye-sensitization exists. Fig. 9b shows the maximum absorption wavelength changes from 554 nm to 539.5 nm, which indicates that RhB just lost one ethyl. However, de-ethylation of RhB was caused by one of the active oxygen species attack on the N-ethyl

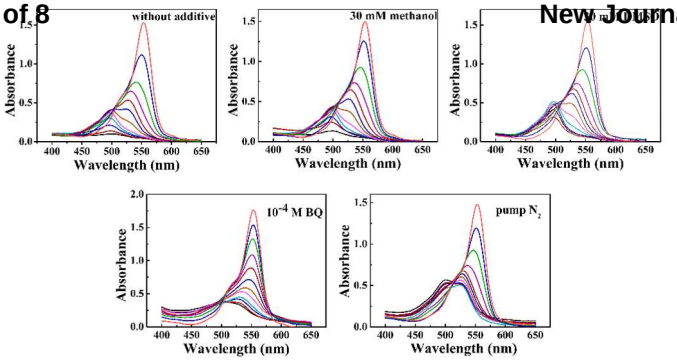

Fig. 10 UV-vis adsorption spectral changes of the RhB solution (10 mg·L^{-1}) over UWAT-1 without additive and with methanol, DMSO, BQ, and nitrogen bubbling as a function of visible light irradiation time.

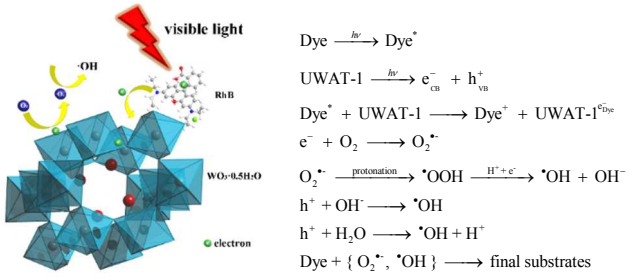

Fig. 11 photocatalytic degradation process diagram of prepared tungsten trioxide hemihydrate.

group. [41] In addition, active oxygen species, like superoxide radicals and hydroxyl radicals, can be formed by photo-generated electron, photo-generated hole, and photo-excited electron in the conduction band of c-WO_3·0.5H_2O which was transferred from RhB*. If there exists dye-sensitization only, and RhB just lost one ethyl that means concentration of active oxygen species is not enough for complete de-ethylation, itindicates that dye-sensitization displays a certain role in photodegradation of RhB.

Secondly, it should be known which active species played a main role. So the photodegradation mechanism experiment of cubic tungsten trioxide hemihydrate was carried out by adding methanol, dimethyl sulfoxide (DMSO), and p-benzoquinone (BQ), which were used as wildly and highly efficient quenchers for holes, hydroxyl radicals, and superoxide radicals, respectively. [42, 43] Fig. 10 shows that adding methanol affects the results of photocatalytic reaction slightly, which indicated that photo-generated hole has played a minor role. When DMSO was added, the processes of intensity of absorption peak decreases and the maximum absorption wavelength of RhB shifts to shorter wavelengths were all subject to a certain degree of inhibition, it inferred that hydroxyl radicals play a certain degree of role not only in de-ethylation process but also in cycloreversion process. The effect of superoxide radicals was also considered by adding BQ. The two processes in reaction of photodegradation were inhibited significantly, the results explained that superoxide radicals play the main role in whole photodegradation process. Because of BQ is colorful, we did a similar experiment of pumping nitrogen. From this supplemental experiment, we got a more pronounced result because of excluding oxygen directly for reducing the formation of superoxide radical, which is more effective than BQ. The above results showed that photogenerated electron is main role during the photodegradation process.

From the above results, we can launch the possible reactions of the degradation process, as shown in Fig. 11.

Conclusions

In summary, cubic tungsten trioxide hemihydrate has been synthesized firstly by simply solvothermal process. Photodegradation of RhB was firstly carried out for investigating its photocatalytic activity, the results demonstrated c-WO_3·0.5H_2O displayed excellent photocatalytic activity. From the photodegradation experiment result of anhydrous c-WO_3 and new c-WO_3·0.5H_2O, it can be known that crystal water played a key role on photocatalytic activity. The c-WO_3·0.5H_2O sample exhibits a long duration even after four cycles of photodegradation. Photolysis experiment results showed that dye-sensitization exists, and superoxide radicals played a main role (generated by photogenerated electron). All results indicated that c-WO_3·0.5H_2O is a promising candidate of tungsten oxide-based photocatalytic materials for pollutant abatement.

Acknowledgements

This work was financially supported by projects of Natural Scie nce Foundation of China (21071036, 21271055) and Natural Sc ience Foundation of Heilongjiang Province (ZD201011).

Notes and references

* *Department of Chemistry, Harbin Institute of Technology, Harbin 150001, P. R. China. E-mail: gchen@hit.edu.cn; Fax: +86-0451-86403117; Tel: +86-0451-86403117*

† *Electronic Supplementary Information (ESI) available [Degradation of RhB by references; UV-vis adsorption spectral changes of the RhB solution; X-ray diffraction (XRD) patterns of tungsten oxides prepared with different pH]*. See DOI: 10.1039/b000000x/

1. S. Sallard, T. Brezesinski and B. M. Smarsly, *J. Phys. Chem. C*, 2007, 111, 7200-7206.
2. S. H. Lee, R. Deshpande, P. A. Parilla, K. M. Jones, B. To, A. H. Mahan and A. C. Dillon, *Adv. Mater.* 2006, 18, 763-766.
3. S. Wang, X. Feng, J. Yao and L. Jiang, *Angew. Chem. Int. Edit.* 2006, 45, 1264-1267.
4. S. Balaji, Y. Djaoued, A. S. Albert, R. Bruning, N. Beaudoin and J. Robichaud, *J. Mater. Chem.* 2011, 21, 3940-3948.
5. S. Yoon, C. Jo, S. Y. Noh, C. W. Lee, J. H. Song and J. Lee, *Phys. Chem. Chem. Phys.* 2011, 13, 11060-11066.
6. W. J. Li and Z. W. Fu, *Appl. Surf. Sci.* 2010, 256, 2447-2452.
7. E. Rossinyol, A. Prim, E. Pellicer, J. Arbiol, F. Hernández-Ramírez, F. Peiró, A. Cornet, J. R. Morante, L. A. Solovyov, B. Tian, T. Bo and D. Zhao, *Adv. Funct. Mater.* 2007, 17, 1801-1806.
8. A. J. T. Naik, M. E. A. Warwick, S. J. A. Moniz, C. S. Blackman, I. P. Parkin and R. Binions, *J. Mater. Chem. A*, 2013, 1, 1827-1833.

9. G. Wang, Y. Ling, H. Wang, X. Yang, C. Wang, J. Z. Zhang and Y. Li, *Energy Environ. Sci.* 2012, 5, 6180-6187.
10. S. S. Kalanur, Y. J. Hwang, S. Y. Chae and O. S. Joo, *J. Mater. Chem. A*, 2013, 1, 3479-3488.
11. D. Chen and J. Ye, *Adv. Funct. Mater.* 2008, 18, 1922-1928.
12. L. Li, M. Krissanasaeranee, S. W. Pattinson, M. Stefik, U. Wiesner, U. Steiner and D. Eder, *Chem. Commun.* 2010, 46, 7620-7622.
13. A. Hameed, M. A. Gondal and Z. H. Yamani, *Catal. Commun.* 2004, 5, 715-719.
14. F. Wang, C. Di Valentin and G. Pacchioni, *J. Phys. Chem. C*, 2012, 116, 8901-8909.
15. L. Zou, Q. Zhong and Q. Liu, Journal of Rare Earths, 2006, 24, 60-66.
16. M. Takeuchi, Y. Shimizu, H. Yamagawa, T. Nakamuro and M. Anpo, *Appl. Catal. B: Environ.* 2011, 110, 1-5.
17. G. Xi, B. Yue, J. Cao and J. Ye, *Chem.-Eur. J.* 2011, 17, 5145-5154.
18. X. An, J. C. Yu, Y. Wang, Y. Hu, X. Yu and G. Zhang, *J. Mater. Chem.* 2012, 22, 8525-8531.
19. M. Seifollahi Bazarjani, M. Hojamberdiev, K. Morita, G. Zhu, G. Cherkashinin, C. Fasel, T. Herrmann, H. Breitzke, A. Gurlo and R. Riedel, *J. Am. Chem. Soc.* 2013, 135, 4467-4475.
20. Y. P. Xie, G. Liu, L. Yin and H. M. Cheng, *J. Mater. Chem.* 2012, 22, 6746-6751.
21. D. Zhang, S. Wang, J. Zhu, H. Li and Y. Lu, *Appl. Catal. B: Environ.* 2012, 123–124, 398-404.
22. J. Shi, G. Hu, R. Cong, H. Bu and N. Dai, *New J. Chem.* 2013, 37, 1538-1544.
23. J. Yu, L. Qi, B. Cheng and X. Zhao, *J. Hazard. Mater.* 2008, 160, 621-628.
24. X. Gao, C. Yang, F. Xiao, Y. Zhu, J. Wang and X. Su, *Mater. Lett.* 2012, 84, 151-153.
25. X. He, C. Hu, Q. Yi, X. Wang, H. Hua and X. Li, *Catal. Lett.* 2012, 142, 637-645.
26. P. Wang, B. Huang, X. Qin, X. Zhang, Y. Dai and M.-H. Whangbo, *Inorg. Chem.* 2009, 48, 10697-10702.
27. R. Nedjar, M. M. Borel and M. H. e. B. Raveau, *Mater. Res. Bull.* 1988.
28. J. R.GUnter, M. Amberg and H. Schmalle, *Mater. Res. Bull.* 1989.
29. P. A. Willlams, P. Leverett, J. L. Sharpe and D. M. Colchester, *Can. Mineral.* 2005.
30. K. H. Chang, C. C. Hu, C. M. Huang, Y. L. Liu and C. I. Chang, *J. Power Sources,* 2011, 196, 2387-2392.
31. X. Li, J. Li, Q. Zhou, Z. Peng, G. Liu and T. Qi, *Metall. Mater. Trans. B*, 2011, 43, 221-228.
32. J. F. Duncan and D. L. Kepert, *J. Chem. Soc. (Resumed)*, 1961, 5317-5325.
33. J. F. Duncan and D. L. Kepert, *J. Chem. Soc. (Resumed)*, 1962, 205-214.
34. J. Chojnacka, *J. Inorg. Nucl. Chem.* 1971, 33, 1345-1363.
35. K. P. Reis, A. Ramanan and M. S. Whittingham, *Chem. Mater.* 1990, 2, 219-221.
36. X. Su, F. Xiao, Y. Li, J. Jian, Q. Sun and J. Wang, *Mater. Lett.* 2010, 64, 1232-1234.
37. H. H. Hatt and A. C. K. Triffett, *Chem. Commun. (London)*, 1965, 439-440.
38. A. R. Butler and I. Hussain, *J. Chem. Soc., Perkin Trans. 2*, 1980, 232-234.
39. J. Z. Su, X. J. Feng, J. D. Sloppy, L. J. Guo and C. A. Grimes, *Nano Lett.* 2011, 11, 203-208.
40. T. Watanabe, T. Takizawa and K. Honda, *J. Phys. Chem.* 1977, 81, 1845-1851.
41. T. Wu, G. Liu, J. Zhao, H. Hidaka and N. Serpone, *J. Phys. Chem. B*, 1998, 102, 5845-5851.
42. T. B. Li, G. Chen, C. Zhou, Z. Y. Shen, R. C. Jin and J. X. Sun, *Dalton T.* 2011, 40, 6751-6758.
43. J. Zhuang, Q. Tian, H. Zhou, Q. Liu, P. Liu and H. Zhong, *J. Mater. Chem.* 2012, 22, 7036-7042.